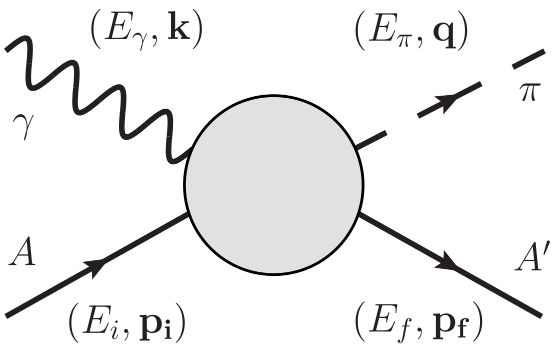

Figure 5.1.: Pion photoproduction. The photon (γ) is absorbed by the nucleus (A) and a pion (π) is produced. The corresponding energies and momenta are given in parenthesis, respectively.

Since the photon requires enough energy to produce a pion with mass $m_{\pi^0} \approx 134.97$ MeV or $m_{\pi^\pm} \approx 139.57$ MeV [37], there is a threshold above which pion production becomes possible. Due to energy and momentum conservation, the threshold photon energy is slightly higher than the bare pion mass and converges to m_π for increasing mass number of the nucleus because the recoil effect becomes negligible. In this work, we concentrate on the pion production at threshold, where the momentum of the produced pion is zero ($\mathbf{q} = \mathbf{0}$). Hence, we deduce from momentum and energy conservation

$$\mathbf{p}_i + \mathbf{k} = \mathbf{p}_f \ , \tag{5.3}$$

$$E_\gamma^{\text{thresh}} = E_f - E_i + m_\pi \qquad \text{with} \quad E_{f/i} = \frac{p_{f/i}^2}{2m_A} \ , \tag{5.4}$$

with the mass of the nucleus m_A, $\boldsymbol{k}$ indicates the photon momentum and $\boldsymbol{p}_i$ ($\boldsymbol{p}_f$) denotes the initial (final) momentum of the nucleus. If we consider the initial nucleus to be at rest ($\mathbf{p}_i = \mathbf{0}$) such that $\mathbf{p}_f = \mathbf{k}$, we obtain for the threshold energy depending on the mass of the nucleus

$$E_\gamma^{\text{thresh}}(m_A) = m_A - \sqrt{m_A^2 - 2m_A m_\pi} \approx m_\pi + \mathcal{O}(m_\pi^2/m_A) \ , \tag{5.5}$$

where we exploited in the last step that $m_\pi \ll m_A$.

Depending on the incoming multipolarity of the photon RL, where R stands for E or M and L denotes the multipole, and the spin of the nucleus S, the outgoing pion-nucleus system can be only in distinct outgoing channels such that angular momentum J and parity are conserved [114]

$$|L \pm S| = J = |l \pm S| \ , \tag{5.6}$$

where l denotes the orbital momentum of the pion relative to the recoiling nucleus. At threshold, the dominant contribution comes from the S-wave multipole E_{0+} of the pion-nucleus system, which corresponds to an incoming $E1$ photon and an orbital momentum of the pion of $l = 0$. Above threshold, where the momentum of the produced pion differs from zero $|\mathbf{q}| > 0$, contributions from P-wave and

Unless otherwise stated, we consistently use the same nuclear wave functions for all calculations throughout Chapter 5.

Note that we use different wave functions than in Ref. [112], which explains the small deviations. Hence, we are consistent with the numerical results. Furthermore, we extend the calculation to ^{6}Li. The same interactions from ChPT are employed as before and the nuclear wave function is calculated by the NCSM for $N_{\max} = 8$. The value for the magnetic moment of ^{6}Li is also consistent with the NCSM result.

5.5.2 One-Nucleon Contribution to the Neutral Pion Photoproduction

We have now all the tools at hand to calculate the one-body contribution to the neutral pion photoproduction at threshold. Following the approach in Ref. [112], we initially compute the transverse form factors $F_T^{S\pm V}$ before stating the final result for the S-wave amplitude E_{0+}^{1N}. This has the advantage that we gain further insights into the neutron and proton properties of the composite nucleus and can directly compare our results with *Lenkewitz et al*. As described in Sec. 5.2, the one-nucleon contribution at LO is illustrated in the first diagram from the left in Fig. 5.2. In this impulse approximation, the nucleons are considered to be coupling independently to the electromagnetic current.

Similar to the magnetic moment calculation, the 1N pion production operator is given by [112]

$$\mathcal{M}_{1N}^{\lambda} = \sum_{i=1}^{A} \mathcal{M}_i^{\lambda} \qquad \text{with} \qquad \mathcal{M}_i^{\lambda} = i\boldsymbol{\epsilon}_T^{\lambda} \cdot \boldsymbol{\sigma}_i \left(\frac{1+\tau_i^z}{2} E_{0+}^{\pi^0 p} + \frac{1-\tau_i^z}{2} E_{0+}^{\pi^0 n} \right) , \tag{5.45}$$

where $\boldsymbol{\epsilon}_T^{\lambda}$ denotes the transverse photon polarization vector for a given polarization λ and $E_{0+}^{\pi^0 p}$, $E_{0+}^{\pi^0 n}$ are the pion production amplitudes off the proton and the neutron, respectively. For the elementary S-wave neutral pion production amplitudes at threshold, we take the predictions from the chiral perturbation theory calculation to order $\mathcal{O}(q^4)$ from Refs. [23, 126]

$$E_{0+}^{\pi^0 p} = -1.16 \times 10^{-3}/M_{\pi^+} \qquad \text{and} \qquad E_{0+}^{\pi^0 n} = +2.13 \times 10^{-3}/M_{\pi^+} , \tag{5.46}$$

given in the usual units. Note that the values above are order $\mathcal{O}(q^4)$ predictions in ChPT, while the chiral order of the LO contribution to the pion production is $\mathcal{O}(q^3)$. There are two reasons for this: First, we want to compare our numerical results for ^{2}H, ^{3}H and ^{3}He with the values of Refs. [26, 113], which use the same predictions as in Eq. (5.46). Second, the order $\mathcal{O}(q^3)$ value for the threshold amplitudes disagrees with the experimentally measured S-wave amplitude at threshold [127]

$$E_{0+}^{\pi^0 p} = (-1.23 \pm 0.08 \pm 0.03) \times 10^{-3}/M_{\pi^+} , \tag{5.47}$$

since the E_{0+} amplitude is only slowly converging in ChPT [23]. The same predictions as in Eq. (5.46) can be derived by averaging the values of Refs. [27, 128]. Furthermore, the E_{0+} amplitudes above are consistent with the results of the chiral unitary approach in Ref. [25]. Since the elementary S-wave amplitudes from ChPT vary by about 5% in Refs. [27, 126, 128], we consequently assign a

5% uncertainty to the E_{0+} amplitudes. Even under consideration of the experimental value above, this seems to be a reasonable assumption. Moreover, this is consistent with the arguments in Ref. [26].

As described in Sec. 5.1 and shown in Eq. (5.8), the S-wave pion production amplitude can be extracted from the expectation value of the pion production operator

$$\left\langle M_J' \middle| \mathscr{M}_{1N}^{\lambda} \middle| M_J \right\rangle_{\Psi} =: 2iE_{0+}^{1N} \left(\boldsymbol{\epsilon}_T^{\lambda} \cdot \boldsymbol{J}\right) = 2i\left(E_{0+}^{\pi^0 p}\frac{F_T^{S+V}}{2} + E_{0+}^{\pi^0 n}\frac{F_T^{S-V}}{2}\right)\left(\boldsymbol{\epsilon}_T^{\lambda} \cdot \boldsymbol{J}\right) . \tag{5.48}$$

First, we calculate the transverse form factors

$$\left\langle M_J' \middle| \hat{O}_{1N}^{\lambda} \middle| M_J \right\rangle_{\Psi} = \left\langle M_J' \middle| \sum_{i=1}^{A} \boldsymbol{\epsilon}_T^{\lambda} \cdot \boldsymbol{\sigma}_i \, \frac{1 \pm \tau_i^z}{2} \middle| M_J \right\rangle_{\Psi} =: F_T^{S\pm V}\left(\boldsymbol{\epsilon}_T^{\lambda} \cdot \boldsymbol{J}\right) . \tag{5.49}$$

The corresponding expectation value is given by

$$\begin{aligned}
\left\langle M_J' \middle| \hat{O}_{1N}^{\lambda} \middle| M_J \right\rangle_{\Psi} &= \sum_{s_i,s_j} \sum_{m_s,m_s'} \int d^3\boldsymbol{k} \int d^3\boldsymbol{k}' \boldsymbol{U}_{s_j,\boldsymbol{k}'m_s'} \boldsymbol{o}^{\lambda}_{m_s'm_t',m_sm_t} \delta^{(3)}(\boldsymbol{k}+\boldsymbol{k}_\gamma-\boldsymbol{k}') \boldsymbol{U}^{\dagger}_{s_i,\boldsymbol{k}m_s} \boldsymbol{\rho}^{1N}_{s_i,s_j} &(5.50)\\
&= \sum_{s_i,s_j} \sum_{m_s,m_s'} \sum_{\boldsymbol{k}} \Delta^3_{\boldsymbol{k}} \boldsymbol{U}_{s_j,(\boldsymbol{k}+\boldsymbol{k}_\gamma)m_s'} \boldsymbol{o}^{\lambda}_{m_s'm_t',m_sm_t} \boldsymbol{U}^{\dagger}_{s_i,\boldsymbol{k}m_s} \boldsymbol{\rho}^{1N}_{s_i,s_j} &(5.51)\\
&= \mathrm{Tr}\left(\boldsymbol{U}\boldsymbol{O}^{\lambda}\boldsymbol{U}^{\dagger}\boldsymbol{\rho}^{1N}_{M_JM_J'}\right) , &(5.52)
\end{aligned}$$

where $\boldsymbol{k}_\gamma$ denotes the photon momentum with $\boldsymbol{\epsilon}_T^{\lambda} \cdot \boldsymbol{k}_\gamma = 0$ and the single-particle operator for the transverse form factors in PW basis reads

$$\boldsymbol{o}^{\lambda}_{m_s'm_t',m_sm_t} = \left\langle \boldsymbol{k} m_s' m_t' \middle| \boldsymbol{\epsilon}_T^{\lambda} \cdot \boldsymbol{\sigma} \frac{(1 \pm \tau^z)}{2} \middle| \boldsymbol{k} m_s m_t \right\rangle , \tag{5.53}$$

where $\pm$ determines the appropriate transverse form factor $F_T^{S\pm V}$.

As explained in Sec. 3.2, the total many-body wave function factorizes into an intrinsic and a CM state

$$|\Psi_{\mathrm{HO}}\rangle = |\Psi_{\mathrm{int}}\rangle \otimes |\Psi_{\mathrm{CM}}\rangle \ . \tag{5.54}$$

Compared to the magnetic moment operator, we have a momentum transfer from the photon to the nucleus in the pion photoproduction. Hence, the center-of-mass (CM) momentum is shifted by the incoming photon momentum $\boldsymbol{k}_\gamma \approx m_{\pi^0}$, cf. Eq. (5.5), due to the recoil of the nucleus. This poses an issue in the NCSM approach since the center-of-mass part of the wave function is expected to remain unchanged for the initial and final wave function.

Therefore, we have to modify our result to account for the shift in the CM momentum. Using

Eq. (5.54), the expectation value above (5.52) reads

$$\langle\Psi_f|\hat{O}^{\lambda}_{1N}|\Psi_i\rangle = \langle\Psi^{\text{int}}_f|\hat{O}^{\lambda}_{1N}|\Psi^{\text{int}}_i\rangle\,\langle\Psi^{\text{CM}}_f|\hat{O}^{\lambda}_{1N}|\Psi^{\text{CM}}_i\rangle = \text{Tr}\left(\boldsymbol{U}\boldsymbol{O}^{\lambda}\boldsymbol{U}^{\dagger}\boldsymbol{\rho}^{1N}_{\Psi_i\Psi_f}\right)\,. \tag{5.55}$$

However, we are only interested in the intrinsic contribution to the pion production. For that reason, we have to divide our result by the CM contribution. In general, the CM state in the NCSM wave function occupies always the HO ground state $|NLM\rangle = |000\rangle$, where we use capital letters for the quantum numbers to indicate the CM state. In the case of the pion production, the overlap of the initial and final CM wave function thus yields

$$\begin{aligned}
\langle\Psi^{\text{CM}}_f|\hat{O}^{\lambda}_{1N}|\Psi^{\text{CM}}_i\rangle = \langle 000|\hat{O}^{\lambda}_{1N}|000\rangle &= \int d^3\boldsymbol{P}'\int d^3\boldsymbol{P}\,\langle 000|\boldsymbol{P}'\rangle\,\delta^{(3)}(\boldsymbol{P}+\boldsymbol{k}_{\gamma}-\boldsymbol{P}')\,\langle\boldsymbol{P}|000\rangle && (5.56)\\
&= \int d^3\boldsymbol{P}\,\langle 000|\boldsymbol{P}+\boldsymbol{k}_{\gamma}\rangle\,\langle\boldsymbol{P}|000\rangle && (5.57)\\
&= \int d^3\boldsymbol{P}\Phi_{00}(|\boldsymbol{P}+\boldsymbol{k}_{\gamma}|)Y^*_{00}(\Omega_{\boldsymbol{P}+\boldsymbol{k}_{\gamma}})\Phi_{00}(|\boldsymbol{P}|)Y_{00}(\Omega_{\boldsymbol{P}}) && (5.58)\\
&= \exp\left(-\frac{1}{4}B^2k^2_{\gamma}\right)\,, && (5.59)
\end{aligned}$$

where $\boldsymbol{P}$ denotes the CM momentum and $B = \sqrt{\hbar/(Am_N\omega)}$ the HO length for the composite system, depending on the number of nucleons A. For ^{3}H, we have to divide our result by a factor of $\langle\Psi^{\text{CM}}_f|\hat{O}^{\lambda}_{1N}|\Psi^{\text{CM}}_i\rangle \approx 0.92$ to obtain only the intrinsic contribution. For increasing A, this factor converges to 1 since the recoil effect becomes negligible. In the case of the magnetic moment, we ignored the CM contribution because $\boldsymbol{k}_{\gamma} = 0$ and the CM part therefore yields $\langle\Psi^{\text{CM}}_f|\hat{O}|\Psi^{\text{CM}}_i\rangle = 1$.

From Eq. (5.49) we can then deduce the general S-wave amplitude. To account for the change in the phase space from the one-nucleon to the A-nucleon system, we have to multiply E^{1N}_{0+} by a kinematical factor [112]

$$K_{1N}(m_A) = \frac{m_N + m_{\pi}}{m_A + m_{\pi}}\frac{m_A}{m_N}\,, \tag{5.60}$$

which depends on the nuclear mass m_A. Thus, the S-wave amplitude for a given nucleus with A nucleons yields

$$E^{1N}_{0+} = \frac{K_{1N}(m_A)}{2}\left(E^{\pi^0 p}_{0+}F^{S+V}_T + E^{\pi^0 n}_{0+}F^{S-V}_T\right)\,. \tag{5.61}$$

At threshold, we obtain non-vanishing amplitudes for all nuclei with spin J unequal to zero. Since the 1N calculation is not computationally exhausting, we can employ large momentum grids so that infrared and ultraviolet errors are negligible. Furthermore, we obtain consistent results for different combinations of initial M_J and final M'_J and varying photon polarizations λ. We also compare the results for different $N_{\max}$ ($e_{\max}$) values and find that the pion production operator is not very sensitive to different HO model spaces. In the case of ^{3}H, we already reach convergence for $N_{\max} = 10$ while the deviation of the $N_{\max} = 2$ from the $N_{\max} = 12$ result is about 5%. A similar behavior is observed for ^{2}H, where the deviation of the $N_{\max} = 2$ from the $N_{\max} = 12$ pion production amplitude is about 7%. Moreover, the results are not very sensitive to different values of $\hbar\omega$ or varying flow parameters in the SRG evolution of the interaction. We expect both errors to be in the single-digit percentage range. Since we want to apply the pion production operator at threshold to a broad range of light nuclei, we have to choose a distinct photon momentum $k_\gamma \approx m_{\pi^0}$ that suits all nuclei. Due to the small deviation from this value induced by the recoil term $\sim k_\gamma/m_A$, we get a systematic error that is below 1% for the nuclei considered here. With these considerations, we estimate the total error to be in range of 5%. Additionally, we have to consider the 5% uncertainty from the ChPT prediction for the single-nucleon amplitudes $E_{0+}^{\pi^0 p/n}$.

As before, our numerical results for ^{3}H and ^{3}He are compared with Ref. [26] and for ^{2}H with Ref. [113] in Tab. 5.2. Taking the uncertainties into account, our values are consistent with the literature.

Table 5.2.: Numerical results of the one-nucleon contribution to the pion production amplitude at threshold for different nuclei. The numbers in parenthesis denote the errors. In the case of two consecutive parentheses, the first error represents the 5% estimation due to different chiral interactions and photon momenta while the second error indicates the uncertainty from the single-nucleon amplitudes. The NCSM calculation is performed for $N_{\max} = 8$ in the case of ^{6}Li and in all other cases for $N_{\max} = 12$. The literature results are taken from Refs. [26, 113].

	our result			literature		
nucleus	F_T^{S+V}	F_T^{S-V}	E_{0+}^{1N} $[10^{-3}/M_{\pi^+}]$	F_T^{S+V}	F_T^{S-V}	E_{0+}^{1N} $[10^{-3}/M_{\pi^+}]$
^{2}H	0.773(39)	0.773(39)	0.40(5)(5)	0.72	0.72	0.37(5) [113]
^{3}H	1.551(78)	0.039(2)	-0.94(5)(5)	1.493(25)	0.012(13)	-0.93(3)(5) [26]
^{3}He	0.041(2)	1.544(77)	1.77(9)(9)	0.017(13)	1.480(26)	1.71(4)(9) [26]
^{6}Li	0.476(24)	0.479(24)	0.26(3)(3)			

Moreover, we calculate the pion production amplitude for ^{6}Li, which has the same nuclear spin structure $J^P = 1^+$ as ^{2}H. By comparing the result of ^{6}Li to the computed values for ^{2}H, ^{3}H, and ^{3}He, we find that the result of ^{6}Li differs significantly from the values for ^{3}H and ^{3}He, while the calculated amplitude of ^{6}Li is only 35% smaller than the value for ^{2}H. Furthermore, the transverse form factors of ^{6}Li are qualitatively similar to those of ^{2}H. The numerical result for ^{6}Li can be explained if we consider that the production amplitude for ^{4}He is zero at threshold and ^{6}Li can be approximated as a composite system of $^6\text{Li} = {}^4\text{He} + {}^2\text{H}$.

As pointed out before, we have to evaluate the pion production operator in HO basis only once for arbitrary nuclei and then multiply it with the appropriate density matrix for the considered nucleus. If we have the nuclear wave function from the NCSM, we can immediately obtain the pion production amplitude at almost zero additional costs. This is the advantage of this density method compared to the Monte Carlo integration of *Lenkewitz et al.*